NASA DEVELOP National Program
Maryland – Goddard

Summer 2024

Nevada Wildland Fires

Mapping Historical Burned Areas and Identifying Drivers of Fuel Load Growth to Inform Desert Tortoise Habitat Management in Southern Nevada

DEVELOP Technical Report

August 9th, 2024

Lucy Hayes (Project Lead)
Hunter Davis
Spencer Harman
Colin Jacobs

Advisors:
Dr. Andrew Feldman, NASA Goddard Space Flight Center, University of Maryland (Science Advisor)
Sean McCartney NASA Goddard Space Flight Center, SSAI (Science Advisor)

Lead:
Isabel Lubitz (Maryland – Goddard)

1. Abstract

Wildfire frequency and intensity in the Mojave desert are increasing, driven by invasive grasses that outcompete native vegetation not well-adapted to wildfire. These grasses, primarily cheatgrass (*Bromus tectorum*) and red brome (*Bromus rubens*), and the wildfires that occur when the grasses ignite, are a serious threat to the critically endangered Mojave desert tortoise (*Gopherus agassizii*). Declining Mojave desert tortoise populations are of great concern to project partners, the Bureau of Land Management Southern Nevada District Office, the US Forest Service's Rocky Mountain Research Station, and the US Department of Agriculture Agricultural Research Service's Arid Lands Ecology Lab, who currently lack the resources for fire recovery studies essential for informed fire and invasive grass management. To address this gap, the team utilized NASA Earth observations including Aqua Moderate Resolution Imaging Spectroradiometer (MODIS), Terra MODIS, Landsat 5 Thematic Mapper (TM), and Landsat 8 Operational Land Imager (OLI), to analyze trends in burned areas over the past 20 years through historic burn maps and to examine fuel load growth drivers, with a focus on invasive vegetation. These historical burn maps revealed a pattern of precipitation anomalies that strongly correlate with higher Normalized Difference Vegetation Index (NDVI) values. Years with significant precipitation and NDVI spikes led to greater fuel load in the dry season and larger burns. Additionally, El Niño years correlated significantly with precipitation anomalies which may provide our partners with insights into burn trends and enable better allocation of fuel load treatment practices. However, while identifying drivers of fuel load growth proved feasible, a lack of in situ data hindered attempts to analyze pre-fire growth of invasive grasses compared with native grasses. Despite this limitation, the project demonstrated the feasibility of using Earth observations for wildfire and habitat management, ultimately benefiting conservation efforts for the Mojave desert tortoise.

Key Terms

Mojave desert tortoise, invasive vegetation, wildland fires, El Niño, dNBR, NDVI, fuel load

2. Introduction

The Mojave desert tortoise (*Gopherus agassizii*) – referred to as the desert tortoise – lives throughout the southwestern United States and northern Mexico, including the Mojave Desert (Murphy et al., 2007). As a keystone species, the Mojave desert tortoise is vital to the ecosystem. For example, many species use the Mojave desert tortoise's burrows, such as the burrowing owl and road runner (The Nature Conservancy, 2021). Despite its importance, the desert tortoise is endangered, with populations declining sharply. Consequently, the Endangered Species Act of 1973 designates Mojave desert tortoise populations located both north and west of the Colorado River as a threatened species (Ruby et al., 2023).

Fires are one of many threats causing the desert tortoise populations to decline in the Mojave. Widespread fires are a relatively new occurrence in these desert scrub habitats (Esque et al., 2003). The frequency and intensity of wildfires are increasing annually across the western half of the United States (Miller et al., 2009). This increased fire risk in the Mojave poses a threat to the tortoise, including direct harm from flames and smoke inhalation (Esque et al., 2003). Wildfires can also affect the species indirectly through the loss of vegetation, serving as cover from predators and high temperatures, as well as acting as a nutrient source for the desert tortoise (Esque et al., 2003).

The frequency and size of fires are significantly correlated with the biomass of non-native plants, especially invasive annual grasses such as red brome (*Bromus rubens*) and cheatgrass (*Bromus tectorum*) (Brooks & Berry, 2006). Invasive grasses support a positive wildfire feedback loop. The invasive grasses are out-competing native plants within the region because the invasive grasses are more fire adapted. The invasive grasses will regrow first within a burned area, which pushes out the native grasses. These invasive grasses burn easier; by pushing out native grasses, the Mojave Desert will see an increase in easily combustible wildfire fuel.

This positive feedback loop of invasive vegetation is a major concern for agencies managing the desert tortoise's habitat. These agencies include the Bureau of Land Management's (BLM) Southern Nevada District Office (SNDO), the US Forest Service's Rocky Mountain Research Station, and the US Department of

Agriculture (USDA) Agricultural Research Service's Arid Lands Ecology Lab. They are responsible for public land and ecosystem management as well as conducting research in the American Southwest. There is a growing need for improved methodologies that rely on remote sensing techniques to address the positive feedback loop of invasive vegetation. To meet this need, we have partnered with these agencies to address this issue. Currently, our partners manage invasive grasses through chemical, mechanical, biological, and manual treatments. However, they lack the resources to conduct post-fire recovery studies that would help them understand invasive vegetation and wildfire dynamics, and support decision-making in fuel load treatment practices.

This project addressed this need by conducting vital post-fire recovery studies. Specifically, we aimed to map twenty years of historic burned areas and identify drivers of fuel load growth, focusing on invasive vegetation. Completing these objectives enabled our partners to analyze trends in post-fire recovery and gain a deeper understanding of factors that increased wildfire risk, thereby contributing to reducing wildfire risk in the desert tortoise habitat. In addition to these objectives, we also assessed the overall feasibility of using remote sensing techniques to enhance invasive grass management.

The study area included much of the Mojave Desert, occupying 25,882 square miles (about the size of West Virginia). The study period spanned from 2004 to 2024. This twenty-year time frame was chosen for several reasons; it allows us to accurately compare anomaly years to the twenty-year average, investigate pre- and post-fire trends of invasive grass regrowth, and explore conditions conducive for fuel load growth across the study area.

Figure 1. Study area map encompassing southern Nevada, southeastern California, northwestern Arizona, and southwestern Utah.

Prior research has shown that remote sensing provides viable techniques for understanding burned areas and conducting fuel load growth analyses. A variety of spectral indices are needed for this work, namely the Normalized Difference Vegetation Index (NDVI), which can be used to evaluate plant phenology. The Normalized Burn Ratio (NBR)(Wasser & Cattau, 2020) can be used to assess the difference between pre-fire

and post-fire vegetation, especially using Landsat data (Keeley, 2009). By using the differenced Normalized Burn Ratio (dNBR), we can see how vegetation and fire levels have changed over time. Given that many external factors such as precipitation, soil type classification, and elevation can impact the growth of invasives, we sought to find what factors drive fuel load growth through Pearson correlation and linear model creation and analysis.

3. Methodology

3.1 Data Acquisition

When collecting data for the historic burn maps, we obtained surface reflectance data from 2004-2024 in Google Earth Engine (GEE) from the Landsat 5 Thematic Mapper (TM) sensor (U.S. Geological Survey, 2012) and Landsat 8 Operational Land Imager (OLI) sensor (U.S. Geological Survey, 2021), using Level 2 Collection 2 Tier 1 surface reflectance scenes for both. We then obtained climate data from the Parameter Elevation Regressions on Independent Slopes Model's (PRISM) daily spatial climate dataset (2004-2024). To validate fire perimeters, we used the Burned Area monthly L3 global 500m image collection from Aqua's Moderate Resolution Imaging Spectrometer (MODIS) sensor. For the fuel load growth model (which includes the Pearson Correlation and Linear Regression Model), we acquired climatic variables from a variety of sources to compare with surface reflectance data acquired from Landsat 5 TM. We acquired 500m resolution data for evapotranspiration from Terra's MODIS sensor, and 500m resolution surface albedo from Terra MODIS Albedo Daily dataset. We also obtained land surface temperature, soil water pH, soil organic carbon, sand, clay and soil water content, and bulk density from OpenLandMap. Furthermore, we acquired the temperature and solar radiation from the ERA5 Land Daily Aggregated dataset. Additional soil-related variables were obtained from the Soil Survey Geographic Database (SSURGO) database from the October 2023 snapshot for the study area, including drainage class, geomorphic description, particle size, soil taxonomic order, water storage (0-25), and water storage (0-150), the latter two being used as a substitute for soil moisture. At the suggestion of our partners, we chose many soil variables as they are influenced by the vegetation and climate of the area (and vice versa). We obtained 30m aspect, elevation, and slope from NASA's Shuttle Radar Topography Mission (SRTM). Finally, we obtained precipitation data from 1981 - 2024 from the Climate Hazards Center InfraRed Precipitation with Station data (CHIRPS). *See Table A1 for more information.*

3.2 Data Processing

3.2.1 Vegetation Indices

The partners were particularly interested in the growth of the invasive grasses in the study area, with a focus on post-fire recovery of these grasses. However, it was only feasible to look at the overall vegetation presence, as there are currently few reliable ways to identify invasive grass species like cheatgrass and red brome from native plants without relying upon ancillary data, and in situ data for our study area which were not available. To visualize post-fire regrowth, we created mean NDVI composites for pre- and post-fire conditions of specific fires within the study area (Hill et al., 2006). We used data from the Near Infrared (NIR) and Red bands of the TM and OLI sensors to calculate NDVI (equation 1; Przyborski, 2000). There are known issues in NDVI accuracy when remotely sensing vegetation in arid landscapes due to spectral signal interference from bare soil (Yang et al., 2017). Knowing this, we also calculated Soil Adjusted Vegetation Index (SAVI; Huete, 1988) as seen in eq. (2). We then compared the different vegetation indices to determine which would be the best at sensing vegetation for the fuel growth analysis. We eventually chose NDVI, as SAVI showed no improvement in imaging vegetation over the conventional NDVI formula.

$$NDVI = \frac{NIR - RED}{NIR + RED} \quad (1)$$

$$SAVI = \left(\frac{NIR - RED}{NIR + RED + \frac{1}{2}}\right) \cdot \frac{3}{2} \quad (2)$$

3.2.2 Fire Indices

We produced the historical burned area maps by calculating the median composite of dNBR (equation 4) for every fire season throughout the study period. For example, to generate a burn map for the 2005 fire season, we took the pre-fire NBR (equation 3) median composite and subtracted it from the post-fire NBR median composite. The pre-fire median composite was filtered from October 2004 to April 2005. Those dates encapsulate the wet season and maximum greening period within the study area. The post-fire composite was filtered from August 2005 to October 2005. The post-fire NBR was after the fire season so that the dNBR maps would identify landscape changes that occurred during the fire season. A positive dNBR signal indicates a burn scar and a negative dNBR response indicates vegetation regrowth. Within the study area, there are two distinct bodies of water, Lake Mead and Lake Mohave. To ensure that only land signals were picked up, we applied a cloud mask to mask out any clouds, cloud shadows, and water. (Carroll et al, 2009). We also incorporated a snow mask to minimize issues of spring snowmelt, which could result in positive dNBR signals. After processing the data in GEE, we exported the data into ArcGIS Pro for further analysis.

$$NBR = \frac{NIR - SWIR}{NIR + SWIR} \tag{3}$$

$$\mathrm{d}NBR = Prefire\ NBR - Postfire\ NBR \tag{4}$$

3.2.3 Standardized Precipitation Index (SPI)

The SPI was adapted to look at precipitation anomalies within the study area from 1981 to 2024. In order to create a three-month Standard Precipitation Index (SPI), we adapted a GEE script from the "Drought Monitoring, Prediction and Projection using NASA Earth Data Systems" ARSET Training (ARSET, 2024). We used the CHIRPS dataset and analyzed precipitation within the study area from 1981-01-01 to 2024-06-01. The three-month SPI was calculated by subtracting the total precipitation by the mean precipitation and dividing by the standard deviation of the precipitation. This created a three-month SPI that compared the precipitation for every three months within our study area during the chosen time period (Schneider et al. 2013).

$$SPI = \frac{(Precipitation - Mean\ Precipitation)}{Standard\ Deviation\ of\ Precipitation} \tag{5}$$

3.2.4 Linear Regression Model

For the fuel load growth analysis, we looked at pre-fire fuel loads for 2005, which was a notable fire year for the study area. Specifically, we used maximum NDVI as a proxy for fuel load growth instead of mean NDVI, to ensure that plants that senesce at different times are represented without a barren soil NDVI value flattening out their signal. Maximum NDVI is a composite of the highest value NDVI pixels over a 3-month pre-fire period. Other temporally bound climatic variables (like temperature, precipitation, etc.) were also carefully compiled from the 3 months prior to the fire (from April to the end of May). The remainder of the variables were static, unchanging with the passage of time, such as elevation. Once the explanatory variables (e.g., the climate and soil relevant variables listed in 3.1) were collected from the study period, we resampled them to the same resolution as the mean precipitation (500 meters). Initially we planned to resample to 30 meters as in the resolution of maximum NDVI, but since many variables were much coarser (500 meters), resampling them into a finer resolution would introduce dramatic jumps in values between pixels that did not reflect the reality of the area. We used the R coding language to compare the explanatory variables as a group against maximum NDVI in a linear regression model. We chose to do this because if each explanatory variable was compared individually with maximum NDVI, and we obtained an R value for each combination instead of one R value representing the group comparison, we would be missing out on the possible interactions between explanatory variables that would explain the plant growth or maximum NDVI better than any individual variable could: there is no way to separate out the effects of precipitation, elevation, etc. from each other in real life, so by including the greatest amount of variables that could possibly explain the

maximum NDVI we would obtain the fullest picture of what drives fuel load growth in this particular time period.

We could not accomplish this without some cleanup of the data first: instead of keeping values outside of the study area as "NA", some variables showed those out-of-bounds areas as "0", which could lead to a false relationship in the linear model. However, we were able to easily replace these 0 values with NA. Additionally, Aspect was a unique explanatory variable in that the data was in degrees at first and needed to be changed to cardinal directions (North 0-45 and 315-360 degrees, East 45-135 degrees, South 135-225 degrees, and West 225-315 degrees). Other categorical variables include Soil Taxonomic Order and Drainage Class, which had 4 and 7 categories respectively that had to be changed from their numerical values (ranging from 1-4 or 1-7) into the descriptive categories to which they corresponded.

3.3 Data Analysis

3.3.1 Visual Analysis of Burn Maps

The historical burn maps were used to visualize burns and vegetation regrowth across the study area over the twenty-year period. Once a map was created, pixel values would be assigned a color that represented a specific class. For example, red represented a possible burn scar, orange/yellow represented predominantly unburnt land, and green represented vegetation regrowth.

3.3.2 Pearson Correlation Analysis

The Pearson correlation analysis served as a preliminary investigation to identify which variables influenced fuel load growth by comparing them directly to our dependent variable, maximum NDVI. To achieve this, we imported several different independent variables (listed in Table B1) into (GEE) and processed them using code that calculated the Pearson correlation coefficient between maximum NDVI and the independent variables. This process was repeated for four different time periods before and after a major fire occurred in July of 2005 to understand which variables correlated with NDVI the most in different time frames. Based on July 2005, we ran the Pearson correlation code for the following time periods: pre-fire short term (3 months before), pre-fire long term (1 year before), post-fire short term (3 months after), and post-fire long term (1 year after).

3.3.3 Linear Regression Model Analysis

The linear regression model focused on the three-month period before the most severe fire in our study period, which occurred in July 2005. Variables chosen differed from the Pearson correlation due to the need for resampling - if we were to use coarse, low-resolution variables like total solar radiation (with a resolution of 1km) the remaining variables would have to be sampled to match which would render data too coarse for use. We dropped the variables with the lowest resolution (such as wind speed) for this reason. Of the variables chosen (listed in Section 3.1), we chose mean precipitation (with a 500m resolution) as the variable all others would be resampled to, since this variable was a necessary inclusion in the analysis and the new coarsest resolution. Max NDVI was the dependent variable, acting as a proxy for "fuel load" or plant growth. We chose which variables to model based on the R-squared and multiple R-squared values, as the closer to 1 those are the more the data is explained by the model. For example, we found that minimum precipitation and maximum snowpack had such a small amount of data within the study area that if we were to use them it would not be an accurate model. The model only takes into account pixels that have an existing (non-NA) value for every variable, so if only one-fourth of the study area was present for the max snowpack variable the model would only take into account that one-fourth area. The partners also helped us to choose what variables to include, emphasizing the importance of categorical variables like aspect, drainage class, and soil taxonomic order. All other variables were numerical. Despite being categorical variables, in the linear regression model each category within the variable acted binary: the presence of that category within the area was assigned a 1, and all other categories were assigned a 0. Thus, categories within variables such as Aspect (North) instead of the entire variable (Aspect) are what can be seen in Table 1, as the subdivided categories can have differing relationships with max NDVI. Unfortunately, due to the limitations of R, not all categories within variables could be seen in the summary. With variables that had more than two categories, often the

categories with a high P-value (meaning a low amount of statistical significance) would not show up on the linear regression model summary, such as Soil Taxonomic Order (Alfisols) that were extremely sparse throughout the study area compared to the other orders. This also occurred with Aspect (East) and Drainage Class (Excessively Drained, Very Poorly Drained, and Moderately Well Drained). Once we created the linear regression model, we analyzed the P-values and the sign of the coefficients for insights on the study area, determining whether the variables had a positive or negative relationship with max NDVI and finding which variables were most highly correlated with our dependent variable, max NDVI.

4. Results & Discussion

4.1 Errors and Uncertainties

While conducting this project, we encountered some sources of error within the results. For the historical burn maps, we were unable to create dNBR maps for 2008 and 2012 due to known issues during Landsat 7 sensor anomalies. Another error that we encountered was related to pixel values on southern facing slopes and a few forests. After calculating the NBR value of the study area, the southern facing slopes and forests were recording a pixel value that indicated a fire, while the true color imagery and historical documents indicated that no fire had occurred in those areas. This was a result of the change in surface reflectance when snow melts. This error was mitigated by adding a snow mask to all the imagery used.

There were also errors and uncertainties within our fuel load growth models. For example, resampling often left an extra row and column that needed to be clipped off despite being at the same resolution, this is a known phenomenon in ArcGIS. Additionally, resampling finer data to a coarser resolution can skew results, and data from the SSURGO database covered less of the study area, so the linear model that includes those parameters is considering a smaller portion of the study area. Lastly, we looked at our parameters for the linear regression model only 3 months before the fire occurrence, whereas the wet season extends further before that three-month period, which may contribute to uncertainty with results.

4.2 Analysis of Results

4.2.1 Historical Burn Maps – Case Study Analysis

As part of the historic burn maps, the partners wanted to focus on pre-fire conditions, post-fire conditions, and post-fire vegetation regrowth. To better understand the pre-fire and post-fire conditions we conducted case studies on active fire seasons. The most active fire season during the study period was the 2005 fire season. We selected a case study plot and control plot to compare pre- and post-fire conditions (Figure 2). Within the case study plot outlined with the red box, there were three separate fires during the 2005 fire season. To complement Figure 2; we created a precipitation and NDVI time series graph that spans from 2003- 2006 (Appendix C).

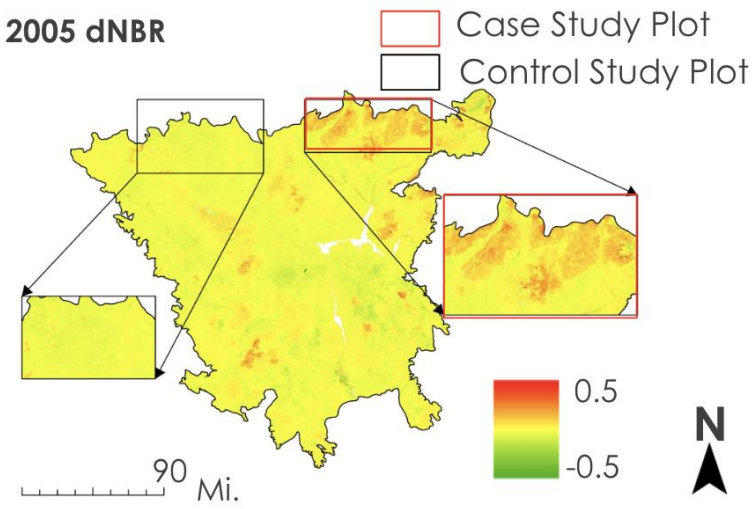

Figure 2. 2005 dNBR map with burned and unburned area

4.2.2 NDVI and Precipitation Time Series

To investigate the pre- and post-fire conditions of the 2005 fires, we plotted monthly precipitation (Figure C1) and NDVI time series (Figure C2) from 2003-2006 within the burned areas. The NDVI time series was visually similar to the precipitation time series – all abrupt increases in NDVI followed precipitation anomalies. During the 2003, 2004, and 2005 wet seasons, there was an increase in NDVI after large precipitation events within the study area. Additionally, during the dry season for all years, there was a decrease in NDVI when the vegetation is senescing before fire season begins. NDVI remains close to 0 during the fires from July to August 2005 and increases up to around 0.05 in the following months, the higher levels signaling regrowth (Figure C2). This helps confirm that regrowth does occur after fire events within the study area.

We also created a monthly precipitation (Figure C3) and NDVI (Figure C4) time series and for the unburned area plot or "control" plot. Like the burned areas, the NDVI time series for unburned areas closely resembled the precipitation time series, with minimal spikes in NDVI that followed the increase in precipitation. The NDVI in these areas remained generally consistent except for a response to the heavy precipitation in the wet season from 2004-2005. The NDVI signal showed some seasonality, but there wasn't enough precipitation to create the large greening events. A lack of growth of vegetation likely influenced why this geographically similar area did not burn while the other plot did.

While visually comparing the precipitation events using a 3-month SPI we noticed that during El Niño years of the Pacific Decadal Oscillation, there was an increase in precipitation anomaly events as demonstrated by the standardized precipitation index (Figure 3). Within the Southern Nevada ecosystem, large precipitation events generally lead to an increase in fuel load due to rapid greening and drying of vegetation. In El Niño years, low-pressure systems from coastal California cause more moist air to funnel over our study area and may lead to increased precipitation. This is likely due to increased rainfall causing more favorable conditions for vegetation regrowth, especially for fast-growing invasive grasses found in our study area (Horn et al, 2015). Additionally, La Niña years tended to have less precipitation than El Niño years which would indicate a lower fuel load year. Knowledge of whether it is an El Niño, La Niña, or moderate year is useful information for our partners as they try to anticipate fuel load growth and its implications on fires for the year.

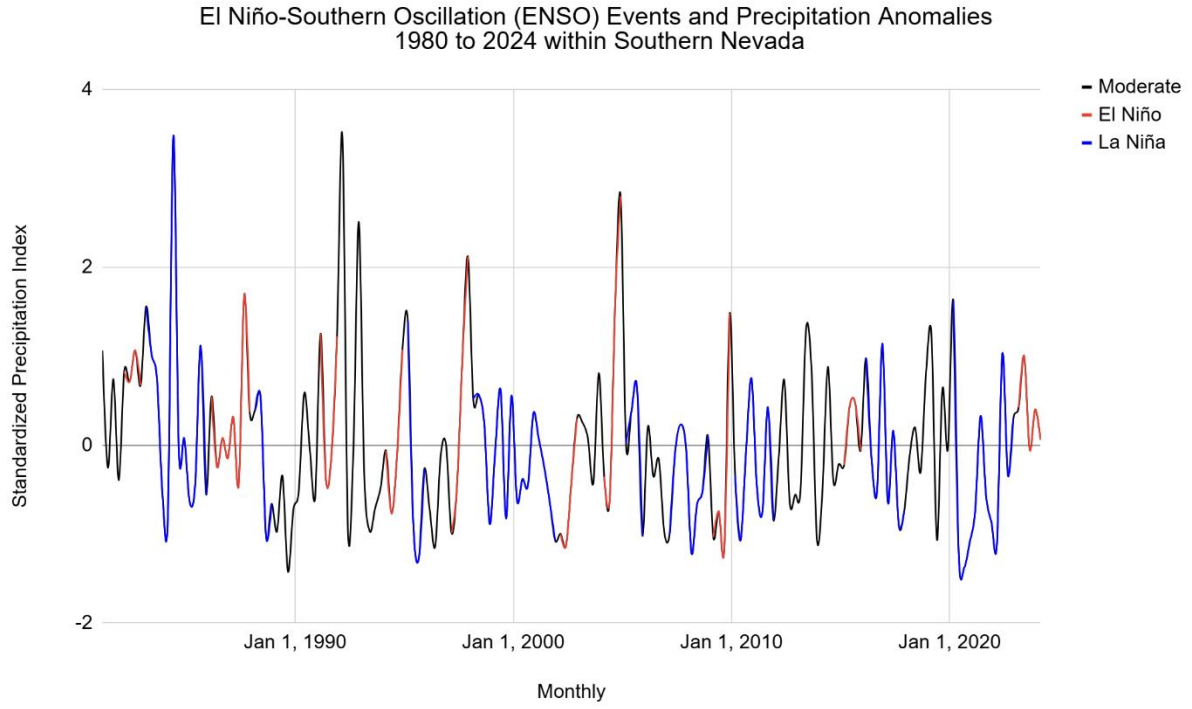

Figure 3. Comparing 3-month standardized precipitation index to El Niño Southern Oscillation (ENSO) Events within Southern Nevada over a 40-year period. Partners were interested in this comparison because they observed that the precipitation anomalies characteristic of El Niño years often drive an increase in fuel load and higher probabilities of fire in the subsequent dry season.

4.2.3 Pearson Correlation Results

The Pearson correlation analysis showed that maximum evapotranspiration, mean albedo, soil water pH, total solar radiation, soil water content, and soil bulk density were consistently the most correlated variables with NDVI over the four time periods, this indicates a strong influence on vegetation health and density. In contrast, minimum precipitation and snow cover were the least correlated variables, likely due to the negligible amount of rain in the desert environment. These results suggest that partners should focus on areas with high values of the strongly correlated variables for fuel load treatments, as these areas are more likely to have higher vegetation density and thus higher fuel loads. By prioritizing these variables, partners can make more informed decisions about where to allocate resources for fuel load treatments.

4.2.4 Linear Regression Model Results

After refining our model, we eventually landed on a combination of variables that best fit the data according to the multiple R values, the highest of which being 0.5083 for the model (Table 1). Variables removed during the refining process included max snowpack, min precipitation, max precipitation, geomorphic description, and particle size (soil). The linear model with these variables included had a multiple R squared value of 0.5983, so the lower value of 0.5083 in the refined version is an improvement. The final linear regression model included maximum NDVI as our dependent variable, with various climatic and soil-related data as our explanatory variables (Table 1). Variables with P-Values lower than 0.001 significance included maximum precipitation, water storage at 0-25cm in the soil, soil organic carbon content, maximum evapotranspiration,

and drainage class (poorly drained soil). The lesser, but still highly correlated variables between 0.001 and 0.01 significance included soil pH, elevation, drainage class (somewhat excessively drained) and drainage class (somewhat poorly drained soils). The somewhat correlated variables between 0.05 and 0.1 significance included aspect (South) and slope. All other variables were not statistically significant enough for us to say that they are correlated to maximum NDVI.

Table 1
Results of Linear Regression Model Analysis (Pre-Fire Short-Term)

Variables and Intercept	**Integer**	**Standard Error**	**T value**	**P value**
Max Evapotranspiration	2.95E-03	8.92E-05	33.054	< 2E-16
Water Storage in Soil (0-25 cm)	2.08E-02	3.38E-03	6.157	8.94E-10
Max Precipitation	-2.46E-03	4.56E-04	-5.39	7.88E-08
Soil Organic Carbon Content	1.25E-02	2.46E-03	5.07	4.33E-07
Drainage Class (Poorly Drained)	2.28E-01	6.86E-02	3.32	9.15E-06
Drainage Class (Somewhat Poorly Drained)	7.96E-02	2.75E-02	2.891	3.89E-06
Drainage Class (Somewhat Excessively Drained)	1.84E-02	6.37E-03	2.893	3.86E-06
Elevation	-1.77E-05	6.06E-06	-2.927	3.47E-06
Soil pH	-2.03E-03	6.78E-04	-2.996	0.003
Slope	-8.33E-04	4.30E-04	-1.937	0.053
Aspect (South)	-7.41E-03	3.95E-03	-1.876	0.061
Max Land Surface Temperature	1.18E-05	9.77E-06	1.206	0.228
Aspect (North)	-6.05E-03	5.72E-03	-1.057	0.291
Drainage Class (Well Drained)	6.25E-03	6.01E-03	1.041	0.298
Aspect (West)	-4.05E-03	3.95E-03	-1.025	0.306
Mean Albedo	6.71E-05	7.46E-05	0.9	0.368
Intercept	-1.12E-01	1.64E-01	-0.686	0.493
Soil Taxonomic Order (Entisols)	2.19E-02	3.67E-02	0.596	0.551
Water Storage in Soil (0-150 cm)	-2.64E-04	5.06E-04	-0.522	0.602
Soil Taxonomic Order (Mollisols)	1.62E-02	3.56E-02	0.456	0.648
Soil Taxonomic Order (Aridisols)	1.07E-02	3.66E-02	0.291	0.771

The results suggest that water availability is an important driver of fuel load growth. Additionally, many results from our Pearson correlation are supported by the linear model, for example maximum evapotranspiration being so highly correlated with max NDVI (likely because of high evapotranspiration during the senescence of plants during the 3-month period prior to the fire). Other variables such as water storage in soil (0-25cm) and soil organic carbon content were both highly correlated with max NDVI, similar to the results of the Pearson correlation (Table B1). Soil organic carbon tends to be higher in areas with more plant growth due to the decomposition of decaying plant matter providing that organic carbon. Finally,

South-facing slopes tend to get the most sun in the Northern Hemisphere (which can promote plant growth or dry the area out depending on the climate), so it is natural that the aspect (South) would be somewhat correlated to NDVI, a proxy of fuel load growth.

4.3 Feasibility & Partner Implementation

With the help of the project outcomes, partners can use remote sensing to help better safeguard the Mojave desert tortoise habitat. The historic regional burn maps help give the partners a historic account of where fires occurred in the past 20 years. Although the use of dNBR mapping in an arid region, like the Mojave Desert, is not as illuminating as it would be in a heavily forested region, our partners will still be able to gather valuable information to analyze plant regrowth and burnt areas with our methods of attaching NDVI and precipitation time-series to each dNBR map throughout the study period. Additionally, partners can use the linear regression model results to understand what group of parameters drove vegetation growth in the pre-fire 2005 period, and the Pearson correlation results to better understand what parameters individually drove vegetation growth in the pre- and post-fire 2005 period. To further validate parameters to monitor, partners could investigate not just the 2005 fire season but other large fire years as well, or change the time of year investigated to the wet season, etc. This same principle applies to the Pearson correlation results. We investigated periods of time 3 months directly pre- and post-fire and 1 year pre- and post-fire, but partners could change the analysis to the wet season or any other period of interest.

Once partners have in situ data on invasive grasses, a spatial analysis or linear regression model taking into account the maximum NDVI of only those invasive grass hotspots might give the partners a better idea of what specifically drives the growth of invasive grasses within the study area. Additionally, historical burn maps could focus on those hotspot areas for a more incisive analysis of the patterns behind invasive grass growth. With the knowledge gained from this project and knowledge of invasive and native grass relationships in the region, the partners may be able to better deem what areas are experiencing more invasive grass growth – compared to native vegetation growth – and decide whether they should chemically treat an area or not.

5. Conclusions

This project had two objectives with varying levels of feasibility. Our first objective, to create historic regional burn maps, was feasible using NASA Earth observations. Our second objective, to create a fuel load growth model, was difficult to accomplish due to a lack of in situ vegetation monitoring data. We were limited to using pre- and post-fire NDVI as the only metric for vegetation growth, a useful proxy but less impactful than it could have been with in-situ measurements of invasive grasses and vegetation in the field. We pivoted so that the fuel load growth analysis would focus on the drivers of all vegetation growth (various environmental and climatic variables) instead of trying to predict specifically invasive grass hotspots. In situ data will be critical for future work on investigating drivers of solely invasive grass growth. Using the Pearson correlation and a linear regression model, we found which variables were most correlated with NDVI, used as a proxy to total fuel load. With this knowledge, the partners can better forecast areas with a higher risk of increased fuel growth.

6. Acknowledgements

We would like to thank everyone involved in the Nevada Wildland Fires Project for their support and guidance, especially our science advisors Dr. Andrew Feldman (NASA Goddard Space Flight Center, University of Maryland) and Sean McCartney (NASA Goddard Space Flight Center, SSAI), as well as our NASA DEVELOP Goddard Space Flight Center Lead Isabel Lubitz. Additionally, we would like to thank our partners Lara Kobelt, Sean McEldery, Benjamin Krupski and Tristan Jamieson at the BLM; Dr. Beth Newingham at the USDA, and Dr. Matt Reeves at the USFS.

This material contains modified Copernicus Sentinel data (2004, 2005, 2006), processed by ESA.

Any opinions, findings, and conclusions or recommendations expressed in this material are those of the author(s) and do not necessarily reflect the views of the National Aeronautics and Space Administration. This material is based upon work supported by NASA through contract 80LARC23FA024.

7. Glossary

Albedo – The proportion of light or radiation that is reflected by a surface.

dNBR – The difference between Pre fire NBR and Post fire NBR. Used to compare pre and post fire conditions.

El Nino Southern Oscillation (ENSO) Events – These events occur due to changing surface temperatures in the central and eastern Pacific Ocean. Warmer surface temperatures indicate an El Nino year, in which milder winters and increased precipitation are expected in the United States. Colder surface temperatures indicate a La Nina year, in which colder winters and decreased precipitation are expected in the United States.

Evapotranspiration (ET) – The process by which water is transferred from the land to the atmosphere by evaporation from the soil and other surfaces and by transpiration from plants.

Fuel Load – Total amount of combustible material in a defined space.

Invasive Vegetation – Invasive vegetation is an introduced species that harms its new environment.

NBR – Is a ratio of the Near Infrared (NIR) and Short-Wave Infrared (SWIR) bands. Used to identify burned areas, burn severity, and healthy vegetation.

NDVI – Is a ratio of the Red and Near Infrared (NIR) bands. It is used as a measurement of vegetation health and greenness.

8. References

AQUA: NASA/LARC/SD/ASDC. (2017). CERES and GEO-Enhanced TOA, Within-Atmosphere and Surface Fluxes, Clouds and Aerosols 1-Hourly Terra-Aqua Edition4A [Data set]. NASA Langley Atmospheric Science Data Center DAAC. Retrieved from https://doi.org/10.5067/TERRA+AQUA/CERES/SYN1DEG-1HOUR_L3.004A

ARSET. (2024). Drought Monitoring, Prediction, and Projection using NASA Earth System Data. NASA Applies Remote Sensing Training Program (ARSET). http://appliedsciences.nasa.gov/get-involved/training/english/arset-drought-monitoring-prediction-and-projection-using-nasa-earth

Brooks, M. L., & Berry, K. H. (2006). Dominance and environmental correlates of alien annual plants in the Mojave Desert, USA. *Journal of Arid Environments, 67*, 100-124. https://doi.org/10.1016/j.jaridenv.2006.09.021

Carroll, M. L., Townshend, J. R., DiMiceli, C. M., Noojipady, P., & Sohlberg, R. A. (2009). A new global raster water mask at 250 m resolution. *International Journal of Digital Earth, 2*(4), 291–308. https://doi.org/10.1080/17538940902951401

Daly, C., Halbleib, M., Smith, J.I., Gibson, W.P., Doggett, M.K., Taylor, G.H., Curtis, J., & Pasteris, P.A. (2008). Physiographically-sensitive mapping of temperature and precipitation across the conterminous United States. *International Journal of Climatology, 28*, 2031-2064. https://doi.org/10.1002/joc.1688

Esque, T. C., Schwalbe, C. R., DeFalco, L. A., Duncan, R. B., & Hughes, T. J. (2003). Effects of desert wildfires on desert tortoise (*Gopherus agassizii*) and other small vertebrates. *The Southwestern Naturalist, 48*(1), 103–111. http://www.jstor.org/stable/3672747

Farr, T.G., Rosen, P.A., Caro, E., Crippen, R., Duren, R., Hensley, S., Kobrick, M., Paller, M., Rodriguez, E., Roth, L., Seal, D., Shaffer, S., Shimada, J., Umland, J., Werner, M., Oskin, M., Burbank, D., & Alsdorf, D.E. (2007). The Shuttle Radar Topography Mission, *Reviews of Geophysics, 45*(2), RG2004.https://doi.org/10.1029/2005RG000183.

Funk, C., Peterson, P., Landsfeld, M., Pedreros, D., Verdin, J., Shukla, S., Husak G., Rowland, J., Harrison, L., Hoell, A., & Michaelsen, J. (2015). The climate hazards infrared precipitation with stations-a new environmental record for monitoring extremes. *Scientific Data, 2*, 150066. https://www.nature.com/articles/sdata201566.

Hall, D. K. & Riggs, G. A. (2016). MODIS/Terra Snow Cover Daily L3 Global 500m SIN Grid, Version 6 [Data Set]. Boulder, Colorado USA. NASA National Snow and Ice Data Center Distributed Active Archive Center. https://doi.org/10.5067/MODIS/MOD10A1.006. Date Accessed 07-31-2024.

Hengl, T. (2018). Long-term MODIS LST day-time and night-time temperatures, sd and differences at 1 km based on the 2000–2017 time series (1.0) [Data set]. Zenodo. https://doi.org/10.5281/zenodo.1420115

Hengl, T. (2018a). Clay content in % (kg / kg) at 6 standard depths (0, 10, 30, 60, 100 and 200 cm) at 250 m resolution (Version v02) [Data set]. https://doi.org/10.5281/zenodo.1476854

Hengl, T. (2018b). Sand content in % (kg / kg) at 6 standard depths (0, 10, 30, 60, 100 and 200 cm) at 250 m resolution (Version v02) [Data set]. https://doi.org/10.5281/zenodo.1476851

Hengl, T. (2018c). Soil bulk density (fine earth) 10 x kg / m-cubic at 6 standard depths (0, 10, 30, 60, 100 and 200 cm) at 250 m resolution (Version v02) [Data set]. Zenodo. https://doi.org/10.5281/zenodo.1475970

Hengl, T. (2018d). Soil pH in H2O at 6 standard depths (0, 10, 30, 60, 100 and 200 cm) at 250 m resolution (Version v02) [Data set]. Zenodo. https://doi.org/10.5281/zenodo.1475459

Hengl, T. & Gupta, S. (2019). Soil water content (volumetric %) for 33kPa and 1500kPa suctions predicted at 6 standard depths (0, 10, 30, 60, 100 and 200 cm) at 250 m resolution (Version v01) [Data set]. Zenodo. https://doi.org/10.5281/zenodo.2629589

Hengl, T. & Wheeler, I. (2018). Soil organic carbon content in x 5 g / kg at 6 standard depths (0, 10, 30, 60, 100 and 200 cm) at 250 m resolution (Version v02) [Data set]. Zenodo. https://doi.org/10.5281/zenodo.1475457

Horn, K.J., Nettles, R. & Clair, S.B.S. (2015). Germination response to temperature and moisture to predict distributions of the invasive grass red brome and wildfire. *Biological Invasions, 17*, 1849–1857. https://doi.org/10.1007/s10530-015-0841-3

Hill, M. J., Roxburgh, S. H., Carter, J. O., & Barrett, D. J. (2006). Development of a synthetic record of fire probability and proportion of late fires from simulated growth of ground stratum and annual rainfall in the Australian tropical savanna zone. *Environmental Modelling & Software, 21*(8), 1214-1229. https://doi-org.byu.idm.oclc.org/10.1016/j.envsoft.2005.06.008

Huete, A. R. (1988). A soil-adjusted vegetation index (SAVI). *Remote Sensing of Environment, 25*(3), 295–309. https://doi.org/10.1016/0034-4257(88)90106-X

Keeley, J. E. (2009). Fire intensity, fire severity and burn severity: A brief review and suggested usage. *International Journal of Wildland Fire, 18*(1), 119. https://doi.org/10.1071/wf07049

LANDFIRE Existing Vegetation Type layer. (2013). U.S. Department of Interior, Geological Survey, and U.S. Department of Agriculture. https://landfire.gov/viewer/

Miller, J. D., Safford, H. D., Crimmins, M., & Thode, A. E. (2009). Quantitative evidence for increasing forest fire severity in the Sierra Nevada and Southern Cascade mountains, California and Nevada, USA. *Ecosystems, 12*(1), 16–32. https://doi-org.byu.idm.oclc.org/10.1007/s10021-008-9201-9

Muñoz Sabater, J. (2019). ERA5-Land monthly averaged data from 1981 to present. Copernicus Climate Change Service (C3S) Climate Data Store (CDS). https://doi.org/10.24381/cds.68d2bb30

Murphy, R. W., Berry, K. H., Edwards, T., & McLuckie, A. M. (2007). A Genetic assessment of the recovery units for the Mojave population of the desert tortoise, *Gopherus agassizii*. *Chelonian Conservation & Biology, 6*(2), 229-251. https://doi.org/10.2744/1071-8443(2007)6

Przyborski, P. (2000). Measuring Vegetation (NDVI & EVI). NASA Earth Observatory, 30, https://earthobservatory.nasa.gov/features/MeasuringVegetation/measuring_vegetation_2.php

Ruby, D. E., Jennings, W. B., Goodlett, G., Spotila, J. R., & Mushinsky, H. R. (2023). Design of roadway barriers to reduce desert tortoise mortality on paved road infrastructure. *Chelonian Conservation & Biology, 22*(1), 103-115. https://doi-org.byu.idm.oclc.org/10.2744/CCB-1533.1

Schaaf, C., Wang, Z. (2015). MCD43A3 MODIS/Terra+Aqua BRDF/Albedo Daily L3 Global - 500m V006 [Data set]. NASA EOSDIS Land Processes Distributed Active Archive Center. Accessed 2024-07-31 from https://doi.org/10.5067/MODIS/MCD43A3.006

Schneider, D. P., C. Deser, J. Fasullo, & Trenberth K. E. (2013): Climate Data Guide Spurs Discovery and Understanding. Eos Trans. AGU, 94, 121–122, https://doi.org/10.1002/2013eo130001

Soil Survey Staff. (2024). Soil Survey Geographic Database (SSURGO). Natural Resources Conservation Service, United States Department of Agriculture. https://www.nrcs.usda.gov/resources/data-and-reports/soil-survey-geographic-database-ssurgo

Running, S., Mu, Q., Zhao, M. (2017). MOD16A2 MODIS/Terra Net Evapotranspiration 8-Day L4 Global 500m SIN Grid V006 [Data set]. NASA EOSDIS Land Processes Distributed Active Archive Center. https://doi.org/10.5067/MODIS/MOD16A2.006

The Nature Conservancy. (2021, May 11). https://www.nature.org/en-us/get-involved/how-to-help/animals-we-protect/desert-tortoise

U.S. Geological Survey Earth Resources Observations and Science Center. (2021). Landsat 8OLI/TIRS Level-1 Surface Reflectance (SR) [Data set]. U.S. Geological Survey. https://doi.org/10.5066/F71835S6

U.S. Geological Survey Earth Resources Observation and Science Center. (2012). Landsat 4-5 TM Level-1 Surface Reflectance (SR) [Data set]. U.S. Geological Survey. https://doi.org/10.5066/P918ROHC

Wasser, L., & Cattau, M. (2020). "Work with the Difference Normalized Burn Index - Using Spectral Remote Sensing to Understand the Impacts of Fire on the Landscape." Earth Data Science - Earth Lab, 1 Mar. 2017, www.earthdatascience.org/courses/earth-analytics/multispectral-remote-sensing-modis/normalized-burn-index-dNBR/.

Yang, Y., Cao, C., Pan, X., Li, X., & Zhu, X. (2017). Downscaling land surface temperature in an arid area by using multiple remote sensing indices with random forest regression. *Remote Sensing, 9*(8), 789. https://doi-org.byu.idm.oclc.org/10.3390/rs9080789

9. Appendices

Appendix A: *Data*

Table A1
Satellites and Datasets

Satellite/Sensor or Dataset	**Processing Level**	**Years**	**Source**
Landsat 5 TM	Collection 2 Tier 1 Raw Scenes	2004-2012	United States Geological Survey (USGS) Earth Explorer (U.S. Geological Survey, 2012)
Landsat 8 OLI	Collection 2 Tier 1 Raw Scenes	2013-2024	USGS Earth Explorer (U.S. Geological Survey, 2021)
LANDFIRE Environmental Vegetation Type (EVT) / (Environmental Vegetation Cover) EVC	N/A	2013-2024	USGS, USDA, United States Forest Service (USFS) (LANDFIRE, 2013)
PRISM Daily Spatial Climate Dataset ANm81	N/A	2004-2024	Parameter-elevation Regressions on Independent Slopes Model (PRISM)/ Oregon State University (Daly, 2008)
MCD66 - Aqua / Moderate Resolution Imaging Spectroradiometer (MODIS)	Burned Area Monthly L3 Global 500m	2004-2024	NASA Land Processes Distributed Active Archive Center (LP DAAC) at USGS Earth Resource Observation and Science (EROS) (Aqua, 2017)
Soil Survey Geographic Database (SSURGO)	N/A	2024	Natural Resources Conservation Service U.S. Department of Agriculture (Soil Survey Staff, 2024)
MOD16A2 - MODIS/Terra Net Evapotranspiration 8-Day L4 Global 500m SIN Grid	N/A	2004-2006	NASA LAADS DACC (Steve, 2015)
MCD43A3.061 - MODIS Albedo Daily 500m	N/A	2004-2006	NASA LP DAAC at the USGS EROS Center (Schaaf, 2015)

OpenLandMap Long-term Land Surface Temperature Daytime Monthly Standard Deviation	N/A	2004-2006	EnvirometriX Ltd (Long-term 2000-2017)
Daymet V4: Daily Surface Weather and Climatological Summaries	N/A	2004-2006	NASA ORNL DAAC at Oak Ridge National Laboratory (Hall, 2016)
OpenLandMap Soil Water Content at 33kPa (Field Capacity)	N/A	2004-2024	EnvirometriX Ltd (Hengl & Gupta, 2019)
OpenLandMap Clay Content	N/A	2004-2024	EnvirometriX Ltd (Hengl, 2018a)
OpenLandMap Sand Content	N/A	2004-2024	EnvirometriX Ltd (Hengl, 2018b)
OpenLandMap Soil Organic Carbon Content	N/A	2004-2024	EnvirometriX Ltd (Hengl & Wheeler, 2018)
OpenLandMap Soil pH in H2O	N/A	2004-2024	EnvirometriX Ltd (Hengl, 2018d)
OpenLandMap Soil Bulk Density	N/A	2004-2024	EnvirometriX Ltd (Funk, 2015)
NASA SRTM Digital Elevation 30m	N/A	2004-2024	NASA / USGS / JPL-Caltech (Muñoz Sabater, 2019)
ERA5-Land Daily Aggregated	N/A	2004-2006	Daily Aggregates: Google and Copernicus Climate Data Store (Farr, 2007)
UCSB-Climate Hazards Center InfraRed Precipitation with Station data (CHIRPS)	N/A	2004-2006	UCSB/CHG (Tomislav, 2018)

Appendix B: *Pearson Correlation Analysis Results*

Table B1
Results of Pearson correlation analysis

Variables	**Pre-Fire (short-term)**	**Pre-Fire (Long-Term)**	**Post-Fire (short-Term)**	**Post-Fire (Long-Term)**
Aspect	-0.066	-0.072	-0.075	-0.039
Elevation	-0.284	-0.120	-0.345	-0.105
Max Albedo	0.448	0.168	0.587	0.141
Max Evapotranspiration	-0.517	-0.618	-0.456	0.085
Max Land Surface Temperature	0.230	0.096	0.381	-0.010
Max Precipitation	-0.222	-0.171	-0.056	no data
Max Snowpack	-0.094	-0.059	-0.076	-0.027
Max Temperature	0.054	-0.028	0.148	no data
Mean Albedo	0.487	0.307	0.598	-0.274
Mean Evapotranspiration	-0.485	-0.459	-0.435	0.0857
Mean Land Surface Temperature	0.271	0.085	0.363	-0.099
Mean Precipitation	-0.210	-0.164	-0.172	0.067
Mean Snowpack	-0.052	-0.019	-0.018	-0.048
Mean Temperature	0.099	-0.045	0.142	0.194
Minimum Albedo	0.478	no data	0.557	-0.096
Minimum Evapotranspiration	-0.311	-0.162	-0.367	0.072
Minimum Land Surface Temperature	0.265	0.070	0.305	0
Minimum Precipitation	0	0	0	no data
Minimum Snowpack	0.007	no data	0.004	-0.006
Minimum Temperature	0.120	-0.057	0.135	-0.112

Slope	-0.238	-0.159	-0.300	-0.289
Soil Bulk Density	0.218	-0.341	0.414	-0.289
Soil Clay Content	-0.097	-0.167	-0.164	-0.083
Soil Organic Carbon Content	-0.292	-0.219	-0.407	-0.183
Soil Sand Content	0.165	-0.048	0.271	-0.081
Soil Water Content	-0.274	-0.232	-0.356	-0.167
Soil Water Ph	0.398	-0.291	0.499	-0.257
Total Solar Radiation	-0.358	-0.237	-0.421	-0.179

Appendix C: *Timeseries Data for 2003-2006*

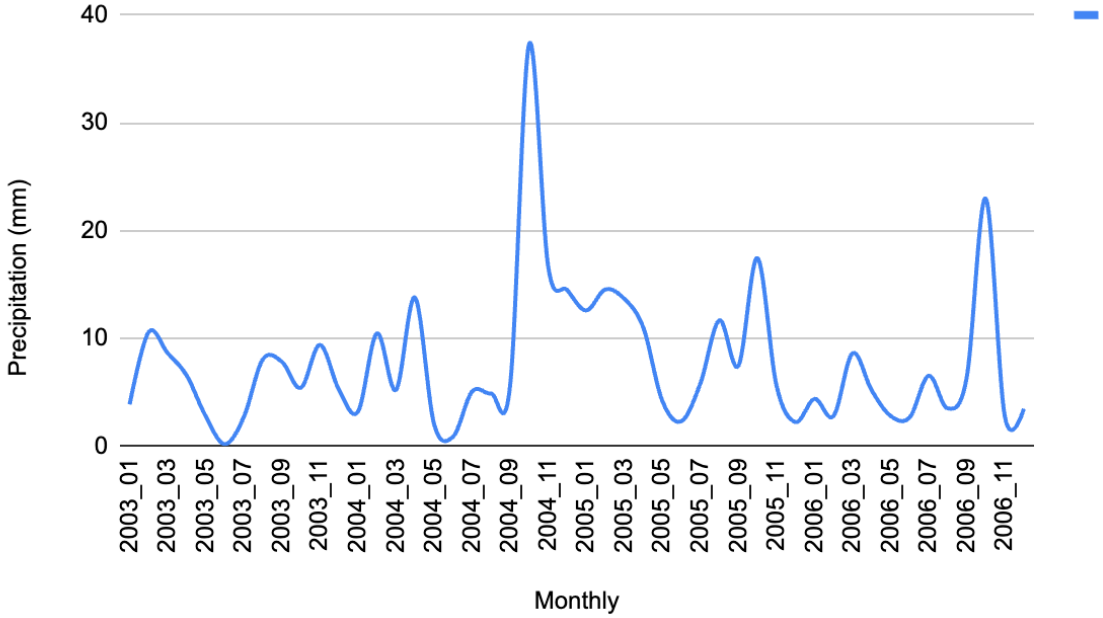

Figure C1. Monthly Precipitation for Burned Area 2003-2006

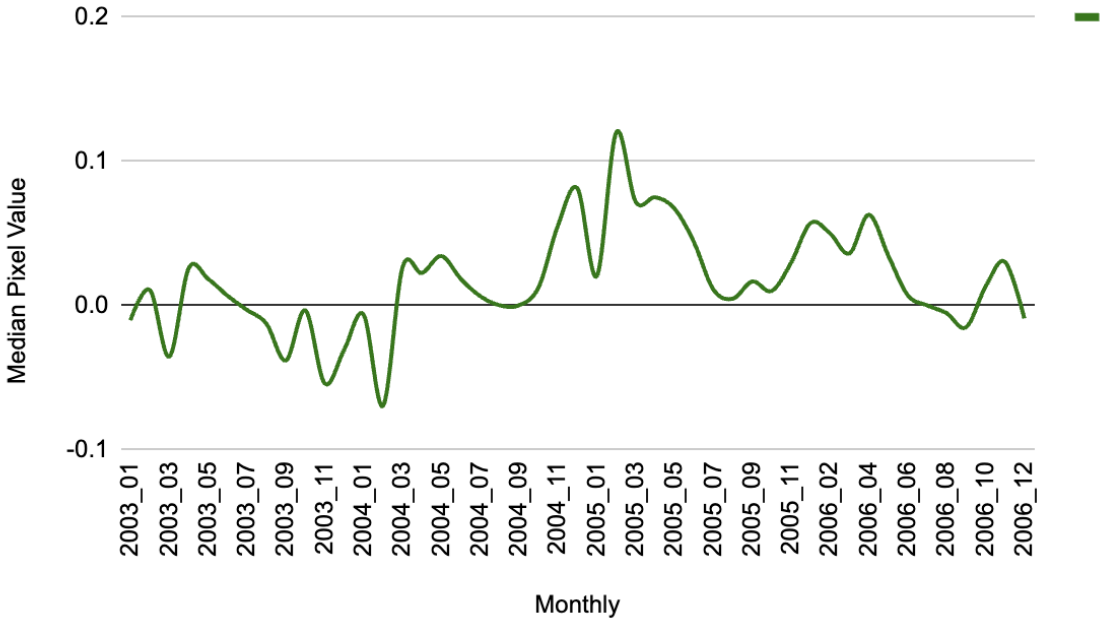

Figure C2. Monthly NDVI for Burned Area 2003-2006

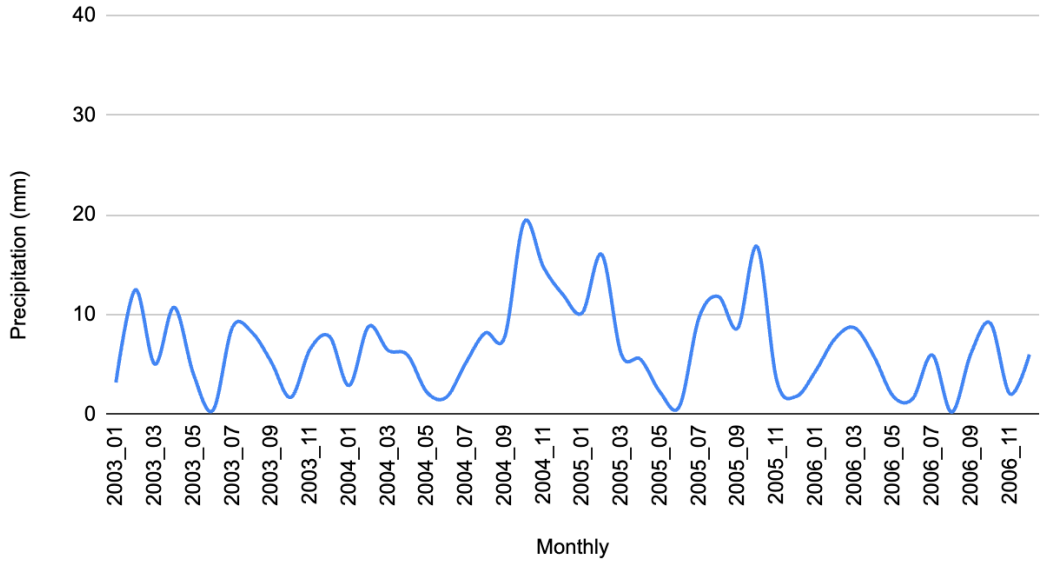

Figure C3. Monthly Precipitation for Unburned Area in 2003 – 2006.

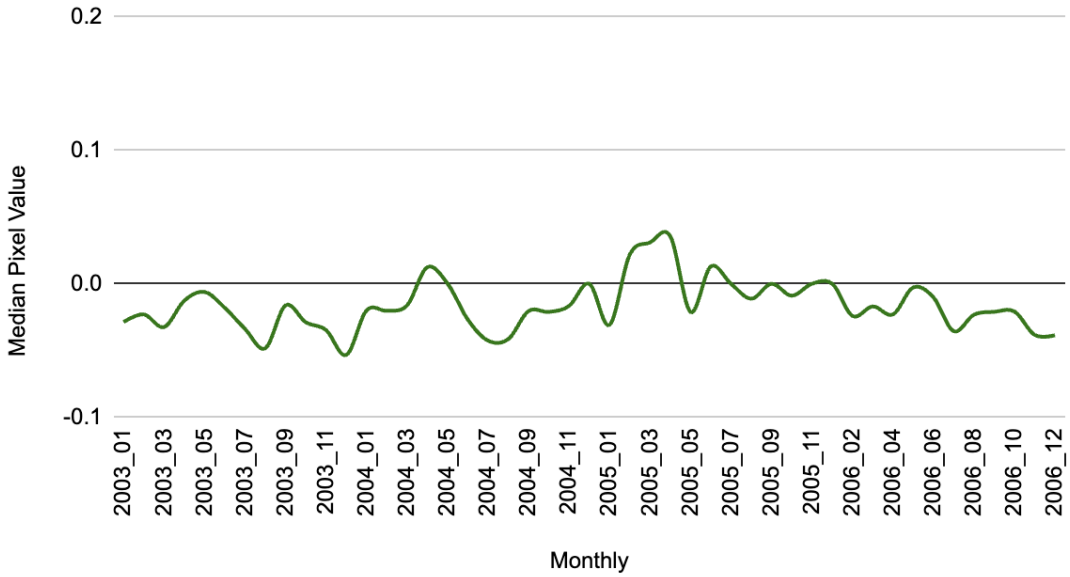

Figure C4. Monthly NDVI for Unburned Area in 2003-2006